

# Lung cancer screening: nodule identification and characterization

Ioannis Vlahos<sup>1</sup>, Konstantinos Stefanidis<sup>2</sup>, Sarah Sheard<sup>3</sup>, Arjun Nair<sup>4</sup>, Charles Sayer<sup>5</sup>, Joanne Moser<sup>1</sup>

<sup>1</sup>St George's NHS Foundation Hospitals Trust and School of Medicine, London, UK; <sup>2</sup>Epsom and St Helier University Hospitals NHS Trust, Epsom, UK; <sup>3</sup>Imperial College Healthcare Trust, London, UK; <sup>4</sup>Guy's and St Thomas' Hospital NHS Foundation Trust, London, UK; <sup>5</sup>Brighton and Sussex University Hospitals Trust, Haywards Heath, UK

*Contributions:* (I) Conception and design: I Vlahos; (II) Administrative support: I Vlahos, J Moser; (III) Provision of study materials or patients: All authors; (IV) Collection and assembly of data: I Vlahos; (V) Data analysis and interpretation: I Vlahos; (VI) Manuscript writing: All authors; (VII) Final approval of manuscript: All authors.

*Correspondence to:* Ioannis Vlahos, MRCP, FRCR. St George's NHS Foundation Trust Hospitals and School of Medicine, London, UK.  
Email: hyperdeepblue@gmail.com.

**Abstract:** The accurate identification and characterization of small pulmonary nodules at low-dose CT is an essential requirement for the implementation of effective lung cancer screening. Individual reader detection performance is influenced by nodule characteristics and technical CT parameters but can be improved by training, the application of CT techniques, and by computer-aided techniques. However, the evaluation of nodule detection in lung cancer screening trials differs from the assessment of individual readers as it incorporates multiple readers, their inter-observer variability, reporting thresholds, and reflects the program accuracy in identifying lung cancer. Understanding detection and interpretation errors in screening trials aids in the implementation of lung cancer screening in clinical practice. Indeed, as CT screening moves to ever lower radiation doses, radiologists must be cognisant of new technical challenges in nodule assessment. Screen detected lung cancers demonstrate distinct morphological features from incidentally or symptomatically detected lung cancers. Hence characterization of screen detected nodules requires an awareness of emerging concepts in early lung cancer appearances and their impact on radiological assessment and malignancy prediction models. Ultimately many nodules remain indeterminate, but further imaging evaluation can be appropriate with judicious utilization of contrast enhanced CT or MRI techniques or functional evaluation by PET-CT.

**Keywords:** Positron emission tomography-computed tomography (PET-CT); lung cancer screening; early lung cancer; nodule detection; missed nodules; nodule characterization; computer-aided detection (CAD); maximum intensity projections (MIPs); reader sensitivity; screening sensitivity; risk models; nodule enhancement study; dynamic contrast CT; dynamic contrast magnetic resonance imaging (MRI)

Submitted Jan 09, 2018. Accepted for publication May 02, 2018.

doi: 10.21037/tlcr.2018.05.02

**View this article at:** <http://dx.doi.org/10.21037/tlcr.2018.05.02>

## Introduction

The identification and characterization of small pulmonary nodules is a pervasive problem in thoracic radiology (1,2). The demonstrated 20% reduction in lung cancer specific mortality in the National Lung Screening Trial (NLST), and the consequent adoption of lung cancer screening has emphasized the importance of nodule detection and evaluation (3,4). Accurate identification of

significant nodules is a prerequisite that can be improved by training, applied CT techniques, and computer-aided detection (CAD). Thereafter, the characterization of identified nodules presents an inherent dichotomy. Nodules identified out of screening programs, either incidentally or as part of cancer or staging evaluations, are evaluated by radiological assessment based principally on their size and morphology. Recommendations for incidentally detected nodules may follow the Fleischner guidelines (5). However,

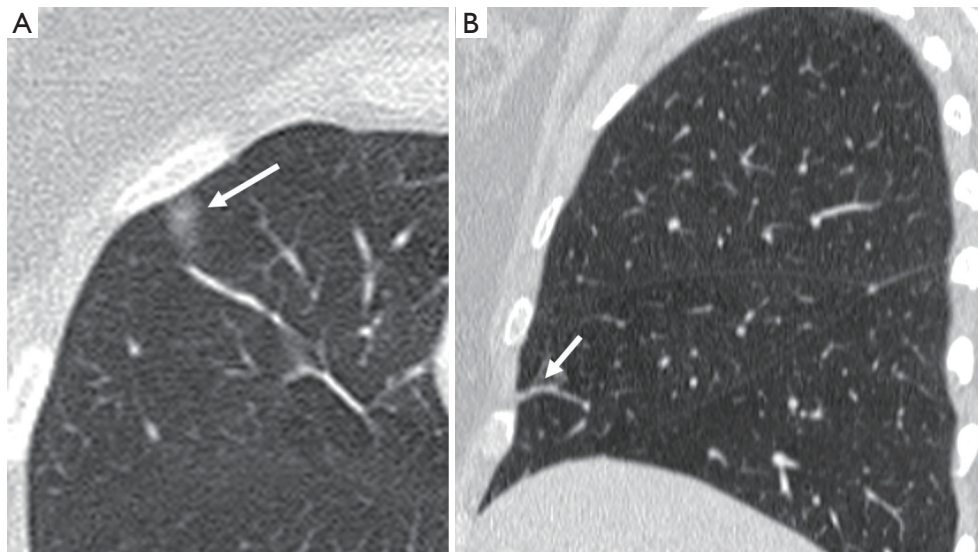


**Figure 1** Simulated subsolid middle lobe nodule (A) is characterized as partial volume averaging of plate atelectasis on sagittal reconstructions (B).

within screening programs, lesion characterization is more protocol constrained, based predominantly on size. Whereas in clinical practice size may be freely determined from linear or volumetric measures depending on available technology, in screening programs this may be protocol dictated. Linear measurements of size are utilised in the Lung-RADS screening protocol implemented in the US (6) but volumetric measurement tools are increasingly prevalent and advocated by the NELSON trial in Europe (7). In practice this dichotomy may be less definitive as patients may move between clinical and screening practice. The radiological morphological interpretation of lesions should retain primacy in lesion characterization regardless of their origination. Designations such as the Lung-RADS “X” characterization retain flexibility for radiologists to record additional interpreted concerning features for malignancy.

This paper reviews the initial detection and evaluation of pulmonary nodules highlighting differences and challenges to this assessment within a screening program. Methodologies for improving the detection of nodules are emphasized and the current understanding of the initial imaging assessment of identified nodules is reviewed. The recommended longer term management and follow-up of identified lesions is outside the scope of this review.

### Nodule definition

An evaluation of the accuracy of nodule identification requires a precise description of what constitutes a nodule.

The Fleischner society defines nodules as a “round opacity at least moderately well marginated” measuring less than 3 cm (8). Therefore, it is clear that not every observable focal opacity is a nodule. Many small focal opacities may simulate nodules, particularly if only reviewed in a single axial plane, but are better characterized on multiplanar images as two-dimensional flat opacities, scars, plate atelectasis or airway abnormalities (Figure 1).

### Nodule detection

The detection performance of pulmonary nodules depends on the reader, the nodule characteristics, the scan technical parameters, and ancillary applied methodologies.

### Reader characteristics

Historically, individual reader nodule detection rates have been variable with inter-observer comparisons hindered by differences in the minimum size definition of nodules, the slice collimation interpreted and how rigorously the ground truth set of all nodules is validated by multiple readers, expert readers, or CAD (9). The sensitivity of human readers for all nodules regardless of size, interpreted with availability of thin-section imaging may be as low as 50% (10). However, the majority of missed lesions are small, measuring less than 5 mm. Larger size thresholds result in predictably higher sensitivities typically in the 75–85% range (11,12). Sensitivity is experience dependent although

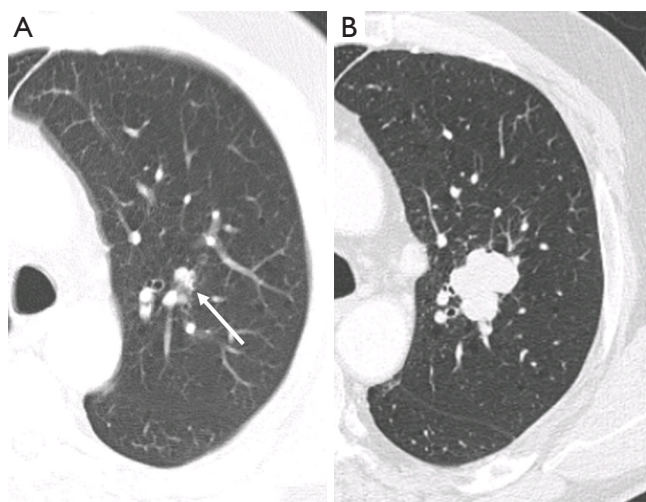


**Figure 2** Inconspicuous central nodule. (A) Missed central 9-mm irregular nodule (arrow) due to non-differentiation from central vessels, a common human reader deficiency; (B) significant growth is noted in the lesion 1 year later with new mediastinal nodes due to progressive adenocarcinoma.

not in a consistent manner, affected by interpretation time, reader fatigue and the extent of abnormalities present that can induce satisfaction of search errors (10-13). A recent study compared experienced radiologists to technologists who underwent two months of training to identify lung nodules >5 mm on low-dose screening studies. Whereas radiologists detected more solid nodules (78% vs. 63%), their part-solid (86% vs. 84%) and ground-glass lesion detection (66% vs. 64%) was not significantly superior. Although technologist interpretations were slower despite being limited to nodule detection alone, such evaluations indicate that nodule observation and detection can be taught and improved in all readers (14).

#### *Nodule characteristics*

In addition to the number of nodules present, individual nodule characteristics that influence detectability include their size, shape, density, margination, location and relationship to vascular or pleural structures (11,12,15). Attachment to vessels or pleural surfaces increases the likelihood of non-detection or misinterpretation as pleural thickening or scarring. Small poorly defined low-density nodules in central locations are more difficult to identify than peripheral larger solid well marginated lesions. The sensitivity for perihilar nodules (37%) in one study was half

that of peripheral nodules (11). Reinforcing this central nodule inconspicuity, in a different study expert readers had only marginally improved sensitivity compared to junior readers (60% vs. 45%) (15) (Figure 2).

#### *Technical characteristics*

The principle technical characteristics that influence the detection of nodules include the absence of motion degradation artefacts, the slice reconstruction thickness, and to a lesser degree the field of view of the reconstruction and image dose. In a hard-copy interpretation study, reduction of slice collimation from 5 to 1.25 mm resulted in detection of 20% more 6–10 mm nodules and 90% more 2–5 mm nodules (16). In clinical practice, however, small nodules may be difficult to differentiate from small vessels on thin sections and large numbers of thin sections contribute to reader fatigue, adversely affecting performance (11,17). A phantom study validated with real nodules determined that the optimal contrast to noise ratio for small nodules is achieved at 4-mm thickness/2-mm overlap although the optimal thickness for nodule characterization was thinner (18). In clinical practice, best performance is likely achieved by the dual availability of relatively thin axial sections for primary interpretation (typically 2.5–3.0 mm), with concomitant availability of contiguous thinner sections (typically 1–1.25 mm) for nodule characterisation and advanced imaging processing.

#### *Multiplanar and 3D techniques*

Coronal and sagittal reconstructions minimally increase sensitivity for nodule detection, but primarily aid in characterizing whether identified opacities are genuine nodules, and characterizing confirmed nodules. Axial overlapping 7–10 mm maximum intensity projections (MIPs) are easily reconstructed and more significantly improve nodule detection (15,19). In particular MIPs improve the detection of small solid nodules, improving discrimination from vessels, and reducing sensitivity differences between senior and junior readers (15,20). Whereas MIPs have been successfully adopted in lung cancer screening programs (21), their use should be complementary rather than replace primary axial review. Seven-millimeter MIPs predictably offered no advantage for the detection of ground-glass lesions (22) and at thicker axial reconstruction thickness MIPs can potentially conceal smaller nodules above or below larger vessels

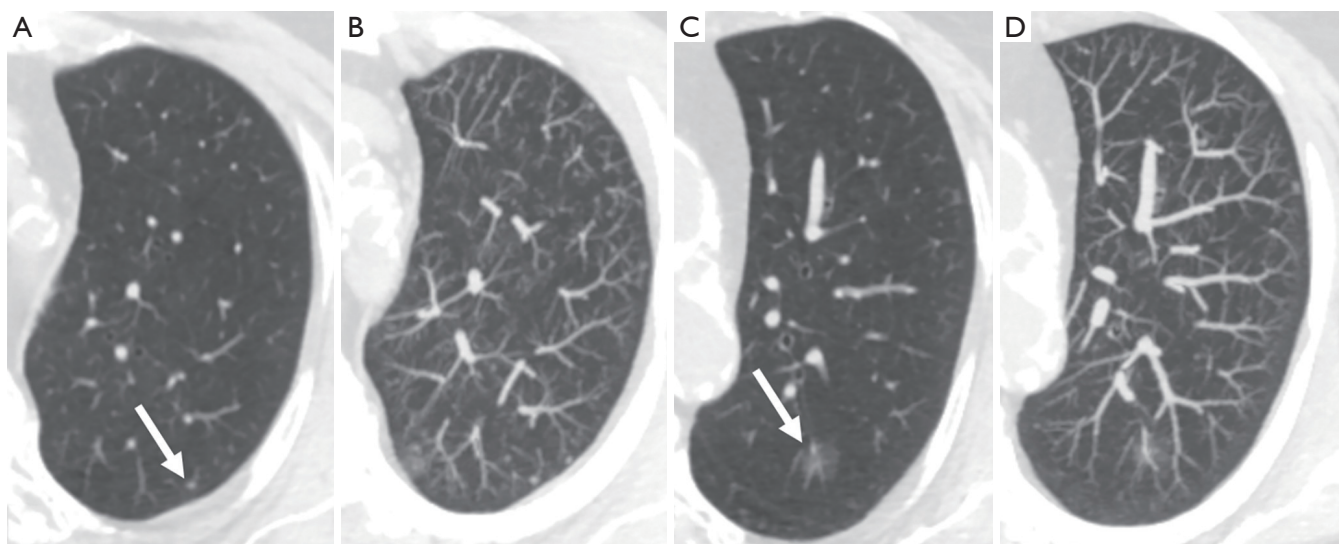


**Figure 3** Two-millimeter axial images (A,C) and corresponding 10-mm MIP images (B,D) in the same patient demonstrate the increased conspicuity of a peripheral solid 2–3 mm nodule at MIP but the reduced conspicuity of a 12-mm ground-glass nodule. MIP, maximum intensity projection.

(Figure 3). The use of MIPs in alternative planes has not been demonstrated to be advantageous over routine axial MIPs (20). Studies evaluating volume rendered thick slab reconstructions provide conflicting evidence as to their value compared to MIPs (19,23).

### CAD

Within screening trials, double reporting is often implemented to improve sensitivity. For small nodules (mean, 3.9 mm) at low-dose CT significant improvement is possible (79% *vs.* 64%) (24). Comparatively, Rubin et al demonstrated that CAD-assisted human reader sensitivity (76%) outperformed both human single reader (50%) and double reporting (63%) (10).

Thin section contiguous data is an essential pre-requisite for optimal CAD implementation. Comparable to human readers, performance depends largely on the nodule type, number and size parameters and the validation of the ground truth reference standard. Progressive CAD sensitivity has been demonstrated with increasing nodule size (54% at 3 mm, 64% at 4 mm, 68% at 5 mm, 76% at 6 mm) (25). Analogous to MIPs much of the incremental benefit to readers occurs with nodules smaller than 5 mm (25,26) which may be less important to detect at screening prevalence rounds but are potentially more important as interval detected nodules. CAD improves all readers,

especially inexperienced readers, but CAD assisted experienced readers remain most sensitive (27).

Validation for the use of CAD comes from varying sources. In a series of non-screening CT studies double read as normal, a CAD system identified unappreciated nodules in 33% of cases (9% >10 mm, 40% 5–9 mm) (28). Early CAD experience with 10mm collimation identified cancers previously missed within screening programs (29,30). More recently, four different CAD systems identified 56–70% of 50 tumors (mean, 4.8 mm) missed on the prevalence round of the I-ELCAP study (31). Within a subset of 400 patients from the NELSON trial that had been double read by human readers, 22% of nodules  $\geq 50$  mm<sup>3</sup> were identified solely by CAD, including one cancer (32).

Whereas a high sensitivity is a desirable intrinsic quality of a superior CAD system, CAD is optimized as a second reader. Hence it is imperative that CAD is implemented in this manner, and not relied on as the primary or sole reader. This principle is highlighted in a phantom study of two readers and three different CAD systems evaluating solid and subsolid nodules  $\geq 5$  mm at varying dose levels. Human readers with CAD assistance had a consistently superior sensitivity (97–99%) than any combination of two CAD systems (85–88%) (33).

Although the advantages of CAD appear self-evident, adoption of CAD has been limited. Barriers to the adoption of CAD include the cost of purchase of dedicated software

or hardware solutions, the historically poor integration into routine picture archiving and communication system (PACS) reading and the impact on reporting times. In lung cancer screening MIPs and CAD provide comparable incremental sensitivity, but MIPs have reduced reporting times and false positives (34,35). Moreover, the inferior CAD identification of subsolid lesions at low-dose CT imaging remains a persistent limitation (26,36). However, whereas human reading ability has limited scope for further improvement CAD performance continues to improve and evolve with advances in neural network and artificial intelligence systems (37). Furthermore, the integrated segmentation and volumetric analysis of CAD systems make their judicious use in screening programs an attractive proposition, particularly in single reading screening environments.

### *Dose considerations*

Low-dose CT imaging in the US prescribes a maximum 3-mGy CTDIvol dose for a standard sized patient (6). In practice, much lower doses can be achieved and may influence human or CAD performance. Lee *et al.* scanned volunteer patients at 6.1, 3.0, 1.52 and 0.76 mGy with conventional filtered back projection reconstruction and found that CAD nodule detection was inferior only at 0.76 mGy (38). The use of iterative reconstruction enables ultra-low dose imaging (~0.25 mGy) while demonstrably preserving the sensitivity of humans in multi-reader studies as well CAD in identifying ground glass nodules in anthropomorphic phantoms (39,40). As low-dose techniques evolve, continuous evaluation is required to ensure that not only are human and CAD reader performances maintained but also that these techniques do not impact the measurement and characterisation of solid and subsolid nodules (41).

### *Screening program sensitivity*

Within reported screening trials the accuracy of individual readers for individual nodules is difficult to discern. High sensitivities (94–95%) for the prevalence rounds of screening trials such as the NLST and NELSON studies typically reference the screening program sensitivity for the detection of cancer (42,43). However, screening protocols influence the detection performance for nodules. With the notable exception of the NLST which implemented single reads per examination, most ongoing screening trials implement double reporting, potentially with additional

CAD interpretation. As most small nodules are benign, the non-visualisation of a single small nodule by a single reader in a screening trial is rarely consequential. Individual nodules may be identified by an alternative human or CAD reader or early case follow-up may be initiated for other identified nodules in the same patient. Subsequent incidence rounds may detect initially missed cancers (except for the UK Lung Cancer Screening Trial which does not implement repeat screening rounds for initially negative studies).

The implementation of minimum reporting size thresholds in prevalence scans (e.g., NLST 4 mm, NELSON 50 mm<sup>3</sup>) also influences perceived sensitivity. The observation that for 30% of positive screens in the NLST prevalence round the average size of the largest solid lesion was <5 mm, but that the malignancy rate in these cases was <0.1% has led to larger solid nodule size thresholds (6 mm) within Lung-RADS to classify positive prevalence screens (44,45). The exclusion of smaller nodules in screening trials, and in clinical screening implementation, improves perceived nodule detection rates by reducing the number of nodules to detect and shifting both human and CAD performance towards easier to detect nodules.

Where individual performance is reported within screening trials this is on a per case evaluation rather than on a per nodule sensitivity evaluation. In an NLST subset study (n=135) the overall multirater k agreement of 16 readers for a positive study (non-calcified nodule ≥4 mm) versus a negative screen (normal study, calcified nodules only or non-calcified <4 mm) was reasonably high (0.64) (46). However, individual pairs of readers demonstrated considerable variation (k =0.40–0.82) with a broad range of studies called positive by individual readers (33–66%). Up to twofold differences in the reader detection of non-calcified nodules measuring 4 mm or greater were apparent. Although detection differences, and interpretation differences (nodule versus non-nodule), accounted for part of this difference, a significant proportion of the difference was attributable to inter-observer differences in nodule size determination at the 4 mm threshold for positivity.

As it is recognized that linear unidimensional measurements are subject to considerable inter-observer variability (47) and rounding measurements may further deviate measurements from true volumetric size (48,49) CAD with integrated volumetric assessment may assist in improving inter-observer variability. In a separate NLST sub-study (n=134) agreement of positive categorisation by seven readers (k =0.53–0.54) improved significantly

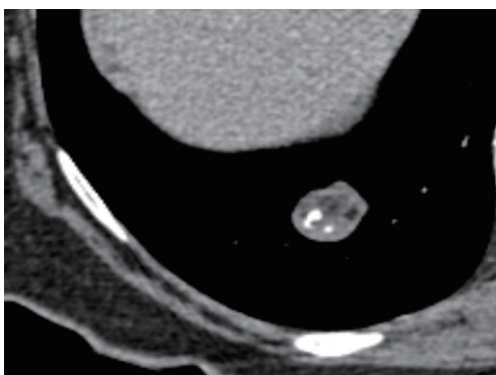


**Figure 4** Typical appearances of a right lower pulmonary hamartoma demonstrating both popcorn calcification and macroscopic fat.

with CAD ( $k = 0.66-0.67$ ) (50). However, the time taken to perform nodule segmentation, check the accuracy of segmentation, perform and record volumetric analysis in large numbers of nodules reflect further practical impediments to routine use even in screening programs.

The most pertinent evaluation of screening nodule detection is reflected in missed nodules within screening programs that ultimately proved to reflect malignancies. The single center Italian COSMOS study reported that 14/175 (8%) of lesions were present on a scan 1 year earlier, but detected on a scan 1 year later at stage II or greater (51). In the NELSON study, following double reporting of all cases by human readers, and of a proportion of studies by CAD, 22 of 61 (36%) interval or post-screen carcinomas were identifiable in retrospect on the immediately prior CT examination (52). Only seven nodules (5 endobronchial, 2 intrapulmonary) were completely not identified. Other pulmonary nodules, hilar, nodal or pleural abnormalities were misinterpreted as benign entities. In the NLST study an analysis of interval cancers occurring after a negative screen but before the next annual screen identified that only 4 of these 44 interval cancers genuinely had no abnormality on the initial scan. In 22 of the 40 identifiable retrospectively identifiable lesions, the lesion was not identified, including five nodules  $\geq 10$  mm, six nodules 4–9 mm and six endobronchial nodules. Similar to the NELSON experience in approximately half of the cases, abnormalities were identified but miscategorised as benign disease (53). In both the NELSON and NLST studies the retrospectively identifiable lesions accounted for less than 10% of the detected tumors but were disproportionately large and advanced at eventual detection.

## Nodule characterization

The characteristics that define benign nodules, and those that increase the risk of malignancy, are well recognised by practising radiologists. However, within screening programs the evaluation of identified nodules requires a meticulous attention to detail, an awareness of the differences between screening identified and symptomatic identified malignancy, a recognition of newly recognized early lung cancer appearances, and of the potential value of risk models.

### Fat

The presence of fat within a lesion is the single most accurate predictor of a benign lesion, usually a benign pulmonary hamartoma (54). The determination of fat within a pulmonary nodule requires the detection of small regions of interest measuring fat density  $< -50$  to  $-75$  Hounsfield units (HU). Fat is most accurately determined on soft kernel reconstruction using thin section imaging (1–2.5 mm), ideally with small field of view reconstructions (12–15 cm), to avoid partial volume average effects of the adjacent low-density lung. As low-dose screening techniques can augment image noise, caution should be exercised in determining the presence of fat attenuation values if imaging is substantially degraded by quantum mottle noise or motion artefacts.

### Calcification

The presence of central punctate, diffuse or lamellated calcification is diagnostic of benign entities, most typically remote granulomatous infections (55) and if the only finding confers a negative screening result.

While eccentric calcifications are statistically also likely benign, occasionally calcified granulomas can become engulfed by an adjacent enlarging malignant soft tissue nodule and, therefore, cannot be considered benign entities at presentation. Dystrophic stippled calcifications are occasionally noted to arise in malignant non-small cell carcinoma and should not be considered benign.

Popcorn-like calcifications are often visualised within hamartomas, which may or may not additionally contain macroscopic fat (*Figure 4*). However, the definition of “popcorn” type calcification is poorly defined and readers may vary in differentiation from eccentric calcifications, which can also occur in carcinoid tumors. Therefore, caution must be exercised in the presence of suspected

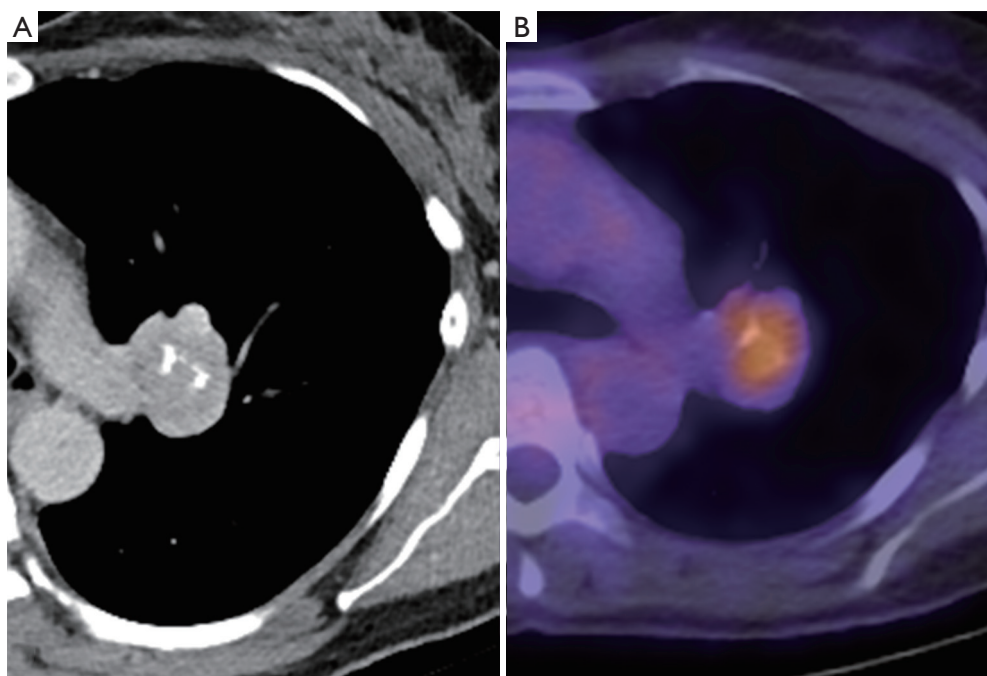


**Figure 5** Central pulmonary lesion demonstrates appearances suggestive of popcorn calcification but without fat (A).  $^{18}\text{F}$ -FDG-PET-CT demonstrates moderately increased metabolic activity (B). Biopsy demonstrated a typical carcinoid, indicating that popcorn type calcification may not be entirely specific for benign lesions.

“popcorn calcification” without fat and further surveillance, or evaluation by  $^{68}\text{Ga}$ -DOTATATE PET-CT or  $^{18}\text{F}$ -FDG PET-CT may be appropriate (56) (Figure 5).

Whereas calcification when definitely present is uniformly recognised, no universal quantitative criterion has been determined across scanner techniques. Early CT recommendations suggested 200 HU was indicative of calcification (55), however, it is important to recognise that the density of nodules can be altered by the use of lower kVp regimens and by iterative reconstruction algorithms (57-59). A visual comparison of a similar lesion density to osseous structures on mediastinal windows is usually sufficient, however, caution should be exercised in small nodules imaged with sharp reconstruction algorithms which can simulate calcification (Figure 6).

#### **Other features favouring benign disease**

Subpleural triangular or ovoid perifissural nodules typically reflect benign intrapulmonary lymph nodes (IPLNs) (60). In a NELSON sub-study such nodules were common, comprising 20% of nodules identified, typically small (mean, 4.4 mm) but occasionally exceeding 1 cm and not

infrequently multiple (61). IPLNs can be also be seen within the lung parenchyma, predominantly at the lung bases, usually round or ovoid, within 2 cm of the pleural surface and demonstrating small septal connections (60,62). Incorporating both typical perifissural and intraparenchymal lymph nodes a British Columbia screening trial demonstrated a slightly higher incidence (28%) of such nodules (63). In both the NELSON and British Columbia experience initial growth, including rapid growth, was not uncommon, but IPLNs subsequently stabilised and none were ultimately malignant.

Characterisation as IPLNs requires care to ensure that the nodules have a broad or obtuse margination to the fissure to exclude peripheral pulmonary nodules, and multiplanar reconstructions can aid determination (Figures 7,8). IPLNs may also appear elongated, an accessory feature of benign disease. Takashima *et al.* defined that nodules with a length/width ratio of  $>1.78$  had a 100% specificity and 62% sensitivity for benign disease (64). IPLNs contain functioning lymphatic tissue and, therefore, in the context of known malignancy or lymphatic disease may represent sites of disease involvement. When incidentally detected such nodules can be dismissed as benign according to

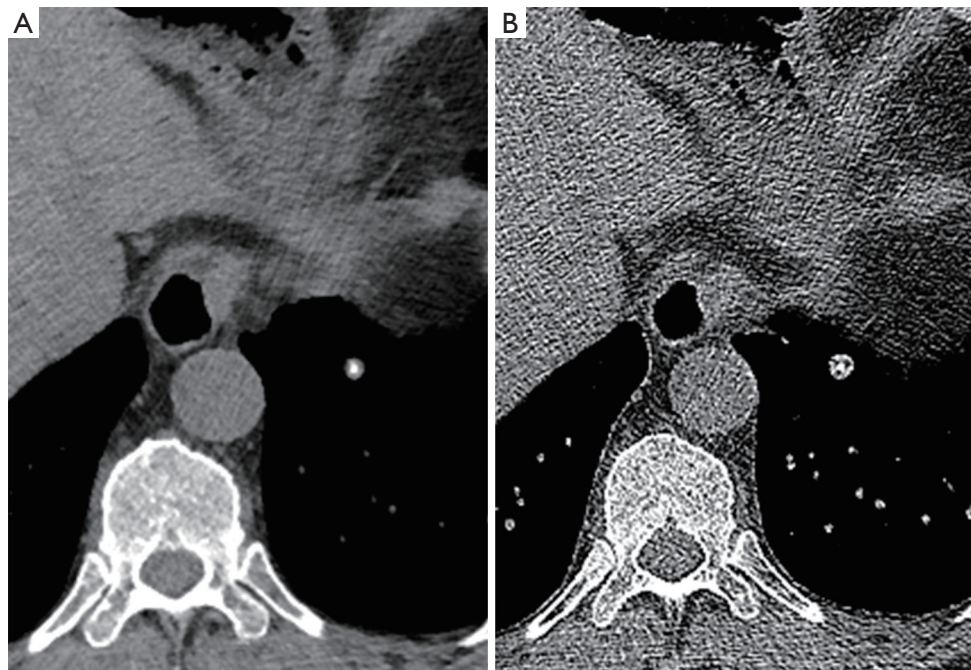


**Figure 6** Small left lower lobe nodule demonstrates central calcification on soft kernel reconstructions consistent with a benign nodule (A). Sharp reconstruction kernel misrepresents calcium distribution, suggesting additional peripheral calcification (B).

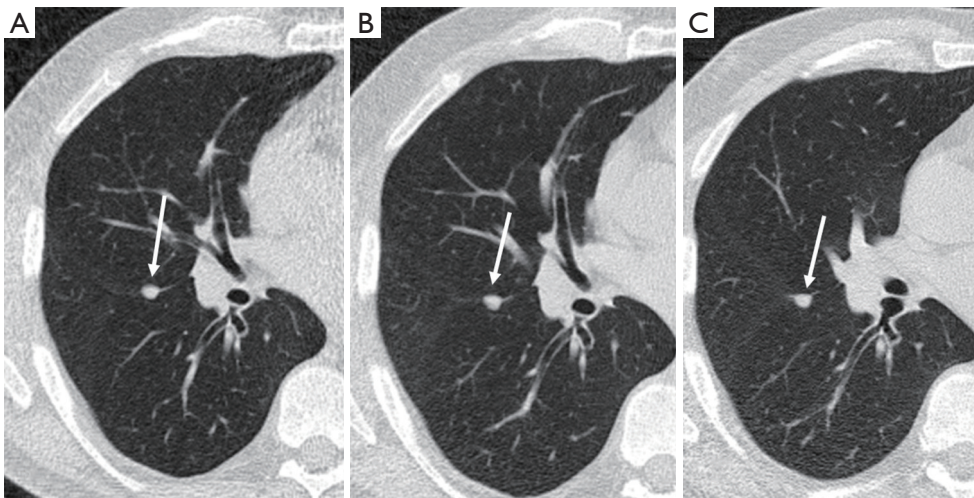


**Figure 7** Broad based smooth nodule with obtuse margins to the adjacent right major fissure shows stability at baseline, 1 and 2 years (A,B,C) consistent with a benign perifissural lymph node.

the Fleischner guidelines (5), however, in the context of screening programs such as Lung-RADS current guidance does not differentiate these lesions from other intrapulmonary nodules (6). This is expected to be modified in a forthcoming version of Lung-RADS.

#### *Features potentially associated with malignancy*

There are no completely specific features of malignant small nodules, despite extensive evaluations of solitary pulmonary nodules in the pre-screening clinical era. Well recognized features such as spiculation, pleural retraction, pleural



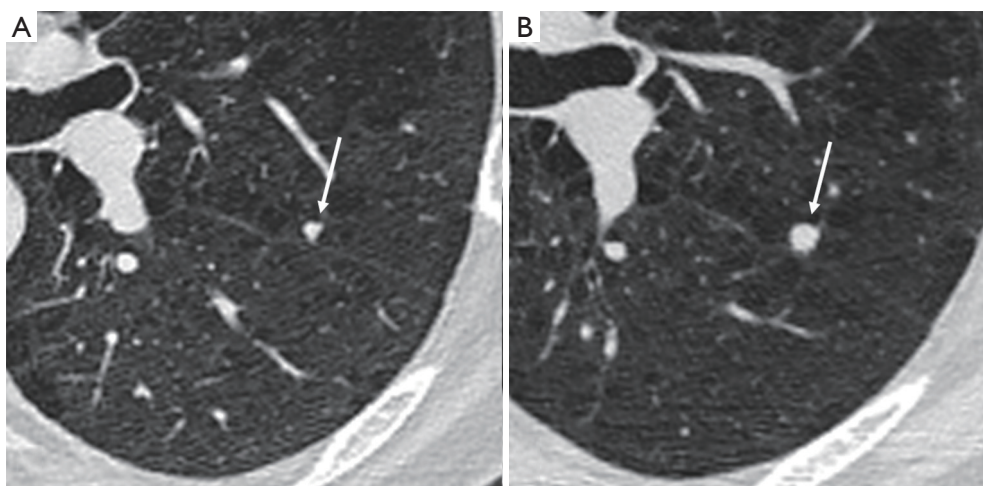


**Figure 8** Small nodule adjacent to the left major fissure demonstrates acute margins to the fissure and does not satisfy criteria for an intrapulmonary lymph node (A). Follow-up at 3 months demonstrates rapid growth of this peripheral pulmonary penile cancer metastasis (B).

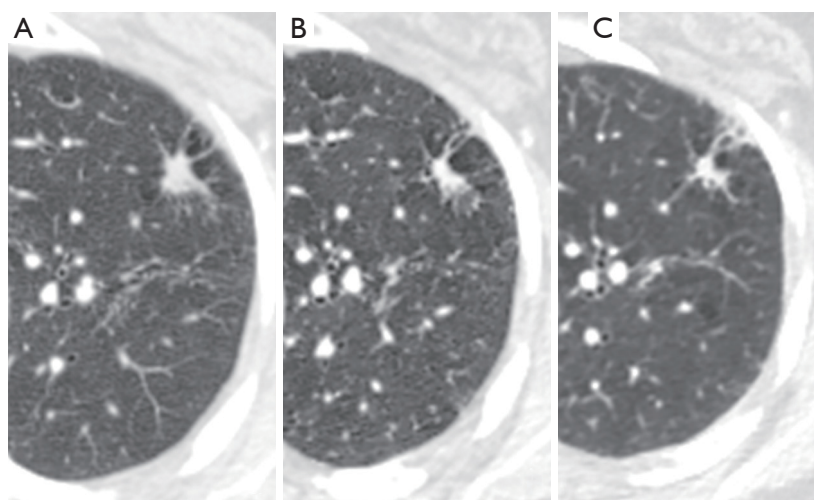


**Figure 9** Spiculated upper lobe nodule with tags to the pleural surface demonstrates multiple features of malignancy at baseline (A), however, regression at 3 (B) and then 6 months (C) highlights that small benign inflammatory lesions can simulate early cancers.

thickening, the bronchus or vessel sign (airway or vessel leading directly to lesion), or part solid characteristics are all associated with a significantly increased risk of malignancy in pulmonary nodules, especially when evaluated at thin section CT (65). Whereas, the presence of one of these features is relatively sensitive in predicting malignancy (91%), specificity is low (57%) as inflammatory lesions can appear similar (*Figure 9*). The identification of subsolid lesions, perhaps accompanied by pseudocavitation can be indicative of adenocarcinoma spectrum lesions, however cavitation itself is also relatively unhelpful. At CT equal

proportions of benign and malignant lesions demonstrate thin or thick walls (66).

In prevalence screening situations the characteristics of detected early stage lung cancers differ compared to non-screen detected lung cancer (42,67). The majority of detected lung cancers are small (10–20 mm) (42,68) (*Figure 10*). As such, whereas the presence of spiculation or irregular margins, remains indicative of malignancy (68), these characteristics are less prevalent and their significance in multivariate analyses appears more limited (69). Small lesion size also impedes the identification of subsolid

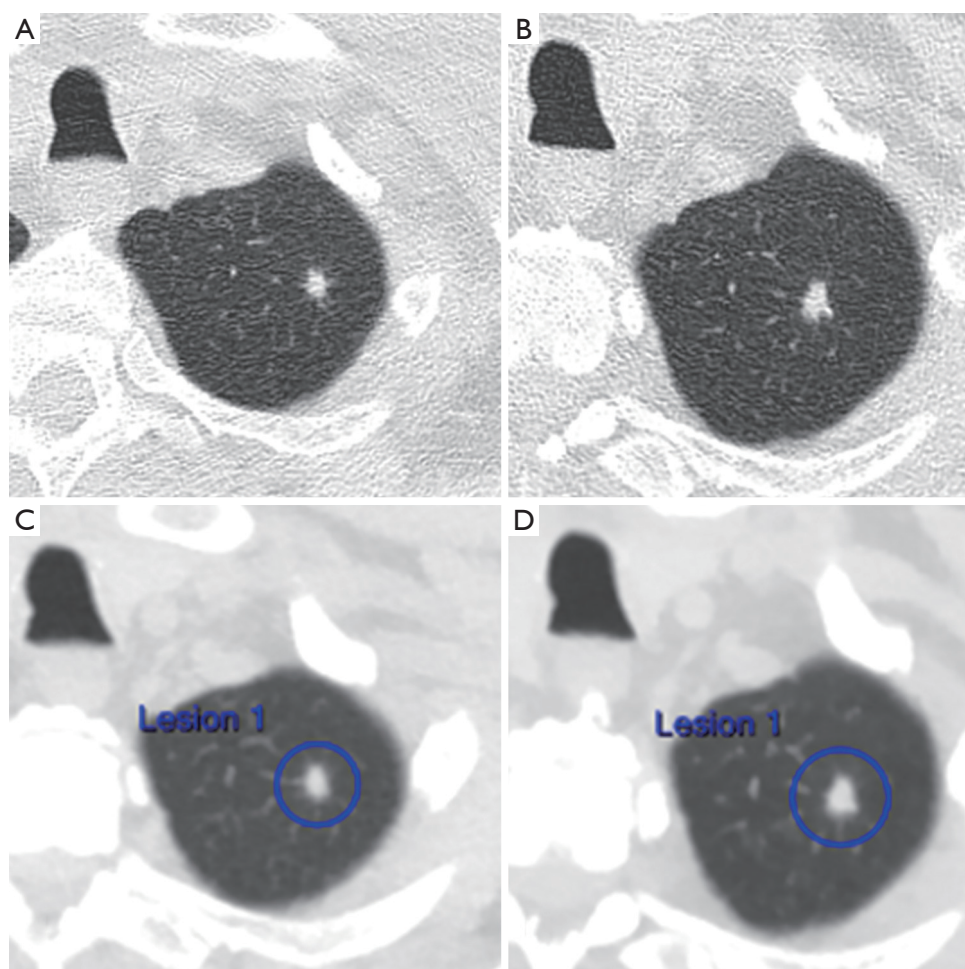


**Figure 10** Screening identifies small cancers that may have limited concerning features at baseline. Left upper lobe nodule measures 5.8 mm at baseline, a borderline positive screen according to Lung-RADS with only 1–2% risk of malignancy (A). Follow-up at 6 months demonstrates growth to 7.5 mm (C). The nodule was detected and assessed by CAD on both occasions (B,D), supporting progression to resection with final diagnosis of a non-mucinous adenocarcinoma. CAD, computer-aided detection.

characteristics, an established risk factor for malignancy. In a NELSON sub-study paired reader agreement for characterization of small lesions as solid, subsolid or part-solid was only moderate ( $k = 0.51$ ). Discordant readings between pairs of readers were present in over a third of cases, predominantly related to the presence or size of a solid component (70). An upper lobe location of screen detected lung cancers appears more common than a lower lobe location. Additionally, smoothly marginated and well-defined nodules are a recognized appearance for a subset of screen detected cancers (67,68). The imaging characteristics of interval or post screen cancers differ from prevalence cancers by inclusion of some new very rapidly evolving aggressive tumors (71). However, the majority of interval

detected screening trial cancers are missed on prior studies related in roughly equal measure to a failure to detect an earlier abnormality or a failure to characterize an identified finding as potentially malignant. A recurrent theme of such misdiagnosis in lung cancer detection relates to emerging recognition of the increased malignant risk of opacities arising adjacent to cystic airspaces.

#### *Early lung cancers associated with cystic airspaces*

In the I-ELCAP study, 26 detected cancers (3.6% of all detected cancers) were identified as abutting or within the wall of a lung cystic airspace (72). Within the NELSON study 5 of 22 interval or post-screen initially missed cancers

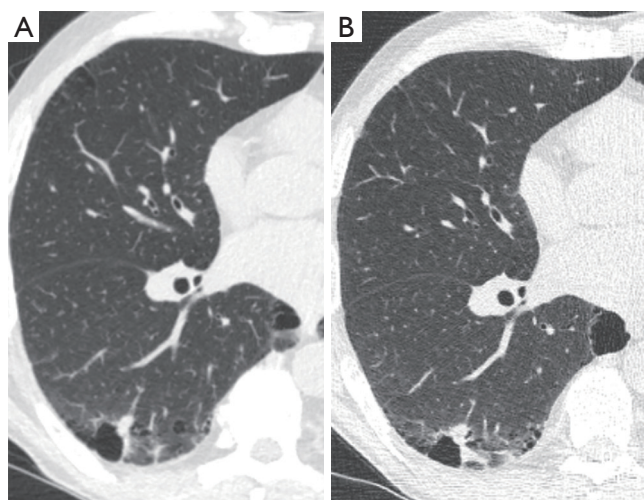


**Figure 11** Baseline image (A) demonstrates minor thickening and nodularity of a peripheral cystic airspace. In view of concern of this morphology, earlier follow-up at 3 months was performed (B). The lesion demonstrated progressive thickening and nodularity around the retracting cystic space a recognised early presentation of lung cancer. Unusually, biopsy demonstrated a non-keratinising squamous cell carcinoma cell type.

similarly reflected lesions arising initially as focal thickening of a bulla (52). In such lesions, progression is appreciated as a gradual increase in thickening or nodularity adjacent to a bulla or cystic airspace which usually demonstrates partial or complete involution (52,72,73) (Figure 11). The CT morphological patterns of cancers arising adjacent to cystic airspaces were initially classified by Maki *et al.*, and then modified by Mascalchi *et al.* although at present no clinical significance is attached to this categorization (74). Histologically, the cystic airspaces can reflect cysts, bullae or dilated airways. Pathologically, the majority of lesions reflect adenocarcinoma, however, the pathogenesis of whether cystic changes induce lung carcinoma or lung cancer induces cystic airspaces remains unclear. From a clinical perspective, these lesions are concerning as a cause of delayed presentation of lung cancer, however, their incidence and best management remains uncertain. Fintelman *et al.* established that 1% of screen detected cancers arose adjacent to a cystic airspace (73). However, in practice a large proportion of thickening adjacent to bullae may be inflammatory; the proportion of these lesions that ultimately evolve to lung cancer remains unknown. Until such data becomes available to inform clinical and screening protocols increased vigilance is advised for such lesions.

### Risk models

As the determination of malignancy within an individual nodule remains an elusive target based on CT morphological features alone, several attempts have been made to incorporate additional clinical parameters into models that can more accurately predict the likelihood of malignancy. In the pre-screening era several models combining radiological features with clinical parameters such as age, sex, race, family history, smoking history, emphysema, and fibrosis were promulgated. Models used either Bayesian analysis (75), or logistic regression such as in the Mayo clinic model (76). While not uniformly superior to physician judgment in assessing the pre-test probability of malignancy, the models tend to counter physician's overestimation of malignancy risk in benign nodules (75,77,78).

However, by virtue of their derivation from a primarily incidental pulmonary nodule cohort with diverse risk profiles, these models may not be ideally suited to evaluating malignancy risk in screening populations. In particular smoking loses its discriminatory value as a significant smoking history is more uniformly present.

More recently, two risk prediction models have been developed by Brock University derived from lung cancer screening data in the Pan-Canadian Early Detection of Lung Cancer Study (Brock or PanCan models) (68). In the so-called parsimonious model, malignant nodules were associated with female sex, increasing nodule size, upper lobe location, and spiculation, while in the full model malignant nodules were also associated with increasing age, family history of lung cancer, emphysema, a lower nodule count, and categorisation as a part-solid nodule. Both models were subsequently validated in separate cohort studies conducted by the British Columbia Cancer Agency and are incorporated into the Lung-RADS 4B category to assist in determining the need for further testing (6). Recently, the discriminatory ability of the Brock model was demonstrated as superior to Lung-RADS categorisation in an analysis of 613 CT studies from the Danish Lung Cancer Screening Trial (79). The evolution of risk models, perhaps accompanied by the advent of complex textural analysis of pulmonary nodules (80) may in the future more accurately refine individual patient management.

### Further imaging techniques for indeterminate nodule evaluation at initial detection

Although the vast majority of screen detected pulmonary

nodules are benign, only a small proportion of nodules demonstrate sufficiently pathognomonic benign features at initial evaluation. The vast majority of nodules will be pathologically indeterminate, and will be categorised according to the screening protocol to direct the timing of future repeat imaging, to assess growth or identify interval new nodules. A small percentage of identified nodules are considered suspicious by size or morphology (e.g., Lung-RADS category 4A, 4B, 4X). In addition to shorter term follow-up or percutaneous biopsy such nodules may benefit from further imaging evaluation at detection by contrast enhanced CT or MRI and PET-CT.

Malignant nodules upregulate endothelial growth factors to support required increases in microscopic vascular density and perfusion (81). Conversely, benign nodules may exhibit relatively limited vascularity. Nodule enhancement studies evaluate enhancement in nodules at five 1-minute intervals following contrast administration. In a multicentre study the absence of enhancement  $>15$  HU was strongly predictive of benignity (negative predictive value 96%) (82). Using alternative peak values of enhancement, Yi *et al.* established that a threshold of enhancement  $>30$  HU, provided sensitivity of 99% and specificity of 54% for the detection of malignancy (81). Similar techniques have been implemented with dual energy CT, where nodule enhancement can be calculated on a single post contrast acquisition. Using a threshold of  $>20$  HU of Iodine related enhancement Chae *et al.* achieved 72% sensitivity and 70% specificity (83). However, the large number of enhancing benign lesions reduces the specificity of enhancement assessment and, therefore, comparative use versus PET-CT is limited. More advanced dynamic evaluations of first pass perfusion have demonstrated promise using both CT and MRI (84). However, in clinical practice the radiation dose constraints of the former, and the technical hurdles for implementation of the latter, have reduced overall adoption of these techniques despite potential comparable or better performance to PET-CT (84).

$^{18}\text{F}$ -FDG-PET is the prevalent physiological imaging technique for indeterminate pulmonary nodules with an established high sensitivity (95%) and intermediate specificity (83%) for the detection of malignancy (85). In a study of 344 patients with solitary pulmonary nodules, PET correctly classified 58% of the benign nodules that had been incorrectly classified as malignant on CT; nodules classified as indeterminate on CT were correctly characterized on PET in over 80% of the cases (86). Lesions are characterized most typically as hypermetabolic either by absolute measurement

of the SUVmax  $>2.5$  or by comparison to reference normal lung tissue or mediastinal blood pool values (86). PET-CT has been successfully integrated into lung cancer screening programs for enlarging nodules with high sensitivity (88% overall, 100% for solid nodules  $>10$  mm) and specificity (93%) using a SUVmax threshold of 2.0 (87).

Recognised limitations of  $^{18}\text{F}$ -FDG-PET include the positivity of some inflammatory changes which reduce specificity. Sensitivity is impacted by a minimum size threshold of 8 mm (88) and the reduced sensitivity in subsolid lesions and low-grade carcinoids (89,90). Dual time point metabolic activity determination has been suggested for lesions with SUVmax  $<2.5$  to assess for progressive metabolic uptake, however, results have been inconsistent (91). Motion degradation near the diaphragms may considerably reduce perceived metabolic activity but may be addressed by new gated PET-CT protocols (92).

## Conclusions

The accurate identification of nodules on low-dose screening CT requires careful attention to reader technique and technical parameters. Reader performance can be improved by commonly available CT reconstruction techniques, or CAD, although users should be cognisant of the limitations of such techniques. In the context of a screening program screening failures relate not only to the non-identification of nodules but also to lack of recognition of the distinct characteristics of early screen detected lung cancers. Nodule evaluation in screening is largely determined by protocols. However, as screening protocols are by necessity consensus methodologies that are infrequently updated, radiologists should use all established and emerging understanding of the morphological characteristics of lesions and risk models to refine screening nodule management.

## Acknowledgements

None.

## Footnote

*Conflicts of Interest:* The authors have no conflicts of interest to declare.

## References

1. Swensen SJ, Jett JR, Sloan JA, et al. Screening for lung

- cancer with low-dose spiral computed tomography. *Am J Respir Crit Care Med* 2002;165:508-13.
2. van Klaveren RV, Oudkerk M, Mali W, et al. Baseline and second round results from the population based Dutch-Belgian randomized lung cancer screening trial (NELSON). *J Clin Oncol* 2008;26:1508.
  3. National Lung Screening Trial Research T, Aberle DR, Adams AM, et al. Reduced lung-cancer mortality with low-dose computed tomographic screening. *N Engl J Med* 2011;365:395-409.
  4. Moyer VA; U.S. Preventive Services Task Force. Screening for lung cancer: U.S. Preventive Services Task Force recommendation statement. *Ann Intern Med* 2014;160:330-8.
  5. MacMahon H, Naidich DP, Goo JM, et al. Guidelines for Management of Incidental Pulmonary Nodules Detected on CT Images: From the Fleischner Society 2017. *Radiology* 2017;284:228-43.
  6. Lung CT Screening Reporting & Data System 2014. Available online: <https://www.acr.org/Clinical-Resources/Reporting-and-Data-Systems/Lung-Rads>
  7. Xu DM, Gietema H, de Koning H, et al. Nodule management protocol of the NELSON randomised lung cancer screening trial. *Lung Cancer* 2006;54:177-84.
  8. Austin JH, Muller NL, Friedman PJ, et al. Glossary of terms for CT of the lungs: recommendations of the Nomenclature Committee of the Fleischner Society. *Radiology* 1996;200:327-31.
  9. Leader JK, Warfel TE, Fuhrman CR, et al. Pulmonary nodule detection with low-dose CT of the lung: agreement among radiologists. *AJR Am J Roentgenol* 2005;185:973-8.
  10. Rubin GD, Lyo JK, Paik DS, et al. Pulmonary nodules on multi-detector row CT scans: performance comparison of radiologists and computer-aided detection. *Radiology* 2005;234:274-83.
  11. Naidich DP, Rusinek H, McGuinness G, et al. Variables affecting pulmonary nodule detection with computed tomography: evaluation with three-dimensional computer simulation. *J Thorac Imaging* 1993;8:291-9.
  12. Rubin GD. Lung nodule and cancer detection in computed tomography screening. *J Thorac Imaging* 2015;30:130-8.
  13. Berbaum KS, Schartz KM, Caldwell RT, et al. Satisfaction of search from detection of pulmonary nodules in computed tomography of the chest. *Acad Radiol* 2013;20:194-201.
  14. Kakinuma R, Ashizawa K, Kobayashi T, et al. Comparison of sensitivity of lung nodule detection between radiologists and technologists on low-dose CT lung cancer screening images. *Br J Radiol* 2012;85:e603-8.
  15. Gruden JF, Ouanounou S, Tigges S, et al. Incremental benefit of maximum-intensity-projection images on observer detection of small pulmonary nodules revealed by multidetector CT. *AJR Am J Roentgenol* 2002;179:149-57.
  16. Fischbach F, Knollmann F, Griesshaber V, et al. Detection of pulmonary nodules by multislice computed tomography: improved detection rate with reduced slice thickness. *Eur Radiol* 2003;13:2378-83.
  17. Ikushima Y, Yabuuchi H, Morishita J, et al. Analysis of dominant factors affecting fatigue caused by soft-copy reading. *Acad Radiol* 2013;20:1448-56.
  18. Hashemi S, Mehrez H, Cobbold RS, et al. Optimal image reconstruction for detection and characterization of small pulmonary nodules during low-dose CT. *Eur Radiol* 2014;24:1239-50.
  19. Kawel N, Seifert B, Luetolf M, et al. Effect of slab thickness on the CT detection of pulmonary nodules: use of sliding thin-slab maximum intensity projection and volume rendering. *AJR Am J Roentgenol* 2009;192:1324-9.
  20. Valencia R, Denecke T, Lehmkuhl L, et al. Value of axial and coronal maximum intensity projection (MIP) images in the detection of pulmonary nodules by multislice spiral CT: comparison with axial 1-mm and 5-mm slices. *Eur Radiol* 2006;16:325-32.
  21. Bastarrika Alemañ G, Domínguez Echávarri PD, Noguera Tajadura JJ, et al. Usefulness of maximum intensity projections in low-radiation multislice CT lung cancer screening. *Radiologia* 2008;50:231-7.
  22. Scholten ET, Mali WP, Prokop M, et al. Non-solid lung nodules on low-dose computed tomography: comparison of detection rate between 3 visualization techniques. *Cancer Imaging* 2013;13:150-4.
  23. Peloschek P, Sailer J, Weber M, et al. Pulmonary nodules: sensitivity of maximum intensity projection versus that of volume rendering of 3D multidetector CT data. *Radiology* 2007;243:561-9.
  24. Wormanns D, Ludwig K, Beyer F, et al. Detection of pulmonary nodules at multirow-detector CT: effectiveness of double reading to improve sensitivity at standard-dose and low-dose chest CT. *Eur Radiol* 2005;15:14-22.
  25. Sahiner B, Chan HP, Hadjiiski LM, et al. Effect of CAD on radiologists' detection of lung nodules on thoracic CT scans: analysis of an observer performance study by nodule size. *Acad Radiol* 2009;16:1518-30.
  26. Marten K, Engelke C, Seyfarth T, et al. Computer-aided detection of pulmonary nodules: influence of nodule characteristics on detection performance. *Clin Radiol*

- 2005;60:196-206.
27. Marten K, Seyfarth T, Auer F, et al. Computer-assisted detection of pulmonary nodules: performance evaluation of an expert knowledge-based detection system in consensus reading with experienced and inexperienced chest radiologists. *Eur Radiol* 2004;14:1930-8.
  28. Peldschus K, Herzog P, Wood SA, et al. Computer-aided diagnosis as a second reader: spectrum of findings in CT studies of the chest interpreted as normal. *Chest* 2005;128:1517-23.
  29. Armato SG 3rd, Li F, Giger ML, et al. Lung cancer: performance of automated lung nodule detection applied to cancers missed in a CT screening program. *Radiology* 2002;225:685-92.
  30. Li F, Arimura H, Suzuki K, et al. Computer-aided detection of peripheral lung cancers missed at CT: ROC analyses without and with localization. *Radiology* 2005;237:684-90.
  31. Liang M, Tang W, Xu DM, et al. Low-Dose CT Screening for Lung Cancer: Computer-aided Detection of Missed Lung Cancers. *Radiology* 2016;281:279-88.
  32. Zhao Y, de Bock GH, Vliegenthart R, et al. Performance of computer-aided detection of pulmonary nodules in low-dose CT: comparison with double reading by nodule volume. *Eur Radiol* 2012;22:2076-84.
  33. Christe A, Leidolt L, Huber A, et al. Lung cancer screening with CT: evaluation of radiologists and different computer assisted detection software (CAD) as first and second readers for lung nodule detection at different dose levels. *Eur J Radiol* 2013;82:e873-8.
  34. Ebner L, Roos JE, Christensen JD, et al. Maximum-Intensity-Projection and Computer-Aided-Detection Algorithms as Stand-Alone Reader Devices in Lung Cancer Screening Using Different Dose Levels and Reconstruction Kernels. *AJR Am J Roentgenol* 2016;207:282-8.
  35. Jankowski A, Martinelli T, Timsit JF, et al. Pulmonary nodule detection on MDCT images: evaluation of diagnostic performance using thin axial images, maximum intensity projections, and computer-assisted detection. *Eur Radiol* 2007;17:3148-56.
  36. Godoy MC, Kim TJ, White CS, et al. Benefit of computer-aided detection analysis for the detection of subsolid and solid lung nodules on thin- and thick- section CT. *AJR Am J Roentgenol* 2013;200:74-83.
  37. Ciompi F, Chung K, van Riel SJ, et al. Towards automatic pulmonary nodule management in lung cancer screening with deep learning. *Sci Rep* 2017;7:46479. Erratum in: *Sci Rep* 2017;7:46878.
  38. Lee JY, Chung MJ, Yi CA, et al. Ultra-low-dose MDCT of the chest: influence on automated lung nodule detection. *Korean J Radiol* 2008;9:95-101.
  39. Rampinelli C, Origgi D, Vecchi V, et al. Ultra-low-dose CT with model-based iterative reconstruction (MBIR): detection of ground-glass nodules in an anthropomorphic phantom study. *Radiologia Medica* 2015;120:611-7.
  40. Nagatani Y, Takahashi M, Murata K, et al. Lung nodule detection performance in five observers on computed tomography (CT) with adaptive iterative dose reduction using three-dimensional processing (AIDR 3D) in a Japanese multicenter study: Comparison between ultra-low-dose CT and low-dose CT by receiver-operating characteristic analysis. *Eur J Radiol* 2015;84:1401-12.
  41. Chen B, Barnhart H, Richard S, et al. Volumetric quantification of lung nodules in CT with iterative reconstruction (ASiR and MBIR). *Med Phys* 2013;40:111902.
  42. National Lung Screening Trial Research Team, Church TR, Black WC, et al. Results of initial low-dose computed tomographic screening for lung cancer. *N Engl J Med* 2013;368:1980-91.
  43. Horeweg N, Scholten ET, de Jong PA, et al. Detection of lung cancer through low-dose CT screening (NELSON): a prespecified analysis of screening test performance and interval cancers. *Lancet Oncol* 2014;15:1342-50.
  44. Gierada DS, Pinsky P, Nath H, et al. Projected outcomes using different nodule sizes to define a positive CT lung cancer screening examination. *J Natl Cancer Inst* 2014;106. doi: 10.1093/jnci/dju284.
  45. Yip R, Henschke CI, Yankelevitz DF, et al. CT screening for lung cancer: alternative definitions of positive test result based on the national lung screening trial and international early lung cancer action program databases. *Radiology* 2014;273:591-6.
  46. Gierada DS, Pilgram TK, Ford M, et al. Lung cancer: interobserver agreement on interpretation of pulmonary findings at low-dose CT screening. *Radiology* 2008;246:265-72.
  47. Revel MP, Bissery A, Bienvenu M, et al. Are two-dimensional CT measurements of small noncalcified pulmonary nodules reliable? *Radiology* 2004;231:453-8.
  48. Li K, Yip R, Avila R, et al. Size and Growth Assessment of Pulmonary Nodules: Consequences of the Rounding. *J Thorac Oncol* 2017;12:657-62.
  49. Heuvelmans MA, Walter JE, Vliegenthart R, et al. Disagreement of diameter and volume measurements

- for pulmonary nodule size estimation in CT lung cancer screening. *Thorax* 2017. [Epub ahead of print].
50. Jeon KN, Goo JM, Lee CH, et al. Computer-aided nodule detection and volumetry to reduce variability between radiologists in the interpretation of lung nodules at low-dose screening computed tomography. *Invest Radiol* 2012;47:457-61.
  51. Veronesi G, Maisonneuve P, Spaggiari L, et al. Diagnostic performance of low-dose computed tomography screening for lung cancer over five years. *J Thorac Oncol* 2014;9:935-9.
  52. Scholten ET, Horeweg N, de Koning HJ, et al. Computed tomographic characteristics of interval and post screen carcinomas in lung cancer screening. *Eur Radiol* 2015;25:81-8.
  53. Gierada DS, Pinsky PF, Duan F, et al. Interval lung cancer after a negative CT screening examination: CT findings and outcomes in National Lung Screening Trial participants. *Eur Radiol* 2017;27:3249-56.
  54. Gaerte SC, Meyer CA, Winer-Muram HT, et al. Fat-containing lesions of the chest. *Radiographics* 2002;22 Spec No:S61-78.
  55. Webb WR. Radiologic evaluation of the solitary pulmonary nodule. *AJR Am J Roentgenol* 1990;154:701-8.
  56. Kayani I, Conry BG, Groves AM, et al. A comparison of 68Ga-DOTATATE and 18F-FDG PET/CT in pulmonary neuroendocrine tumors. *J Nucl Med* 2009;50:1927-32.
  57. Bhalla M, Shepard JA, Nakamura K, et al. Dual kV CT to detect calcification in solitary pulmonary nodule. *J Comput Assist Tomogr* 1995;19:44-7.
  58. Goodsitt MM, Chan HP, Way TW, et al. Accuracy of the CT numbers of simulated lung nodules imaged with multi-detector CT scanners. *Med Phys* 2006;33:3006-17.
  59. Lo P, Young S, Kim HJ, et al. Variability in CT lung-nodule quantification: Effects of dose reduction and reconstruction methods on density and texture based features. *Med Phys* 2016;43:4854.
  60. Hyodo T, Kanazawa S, Dendo S, et al. Intrapulmonary lymph nodes: thin-section CT findings, pathological findings, and CT differential diagnosis from pulmonary metastatic nodules. *Acta Med Okayama* 2004;58:235-40.
  61. de Hoop B, van Ginneken B, Gietema H, et al. Pulmonary perifissural nodules on CT scans: rapid growth is not a predictor of malignancy. *Radiology* 2012;265:611-6.
  62. Oshiro Y, Kusumoto M, Moriyama N, et al. Intrapulmonary lymph nodes: thin-section CT features of 19 nodules. *J Comput Assist Tomogr* 2002;26:553-7.
  63. Ahn MI, Gleeson TG, Chan IH, et al. Perifissural nodules seen at CT screening for lung cancer. *Radiology* 2010;254:949-56.
  64. Takashima S, Sone S, Li F, et al. Small solitary pulmonary nodules (< or =1 cm) detected at population-based CT screening for lung cancer: Reliable high-resolution CT features of benign lesions. *AJR Am J Roentgenol* 2003;180:955-64.
  65. Seemann MD, Seemann O, Luboldt W, et al. Differentiation of malignant from benign solitary pulmonary lesions using chest radiography, spiral CT and HRCT. *Lung Cancer* 2000;29:105-24.
  66. Honda O, Tsubamoto M, Inoue A, et al. Pulmonary cavitory nodules on computed tomography: differentiation of malignancy and benignancy. *J Comput Assist Tomogr* 2007;31:943-9.
  67. Horeweg N, van der Aalst CM, Thunnissen E, et al. Characteristics of lung cancers detected by computer tomography screening in the randomized NELSON trial. *Am J Respir Crit Care Med* 2013;187:848-54.
  68. McWilliams A, Tammemagi MC, Mayo JR, et al. Probability of cancer in pulmonary nodules detected on first screening CT. *N Engl J Med* 2013;369:910-9.
  69. Xu DM, van Klaveren RJ, de Bock GH, et al. Limited value of shape, margin and CT density in the discrimination between benign and malignant screen detected solid pulmonary nodules of the NELSON trial. *Eur J Radiol* 2008;68:347-52.
  70. van Riel SJ, Sanchez CI, Bankier AA, et al. Observer Variability for Classification of Pulmonary Nodules on Low-Dose CT Images and Its Effect on Nodule Management. *Radiology* 2015;277:863-71.
  71. Walter JE, Heuvelmans MA, Oudkerk M. Small pulmonary nodules in baseline and incidence screening rounds of low-dose CT lung cancer screening. *Transl Lung Cancer Res* 2017;6:42-51.
  72. Farooqi AO, Cham M, Zhang L, et al. Lung cancer associated with cystic airspaces. *AJR Am J Roentgenol* 2012;199:781-6.
  73. Fintelmann FJ, Brinkmann JK, Jeck WR, et al. Lung Cancers Associated With Cystic Airspaces: Natural History, Pathologic Correlation, and Mutational Analysis. *J Thorac Imaging* 2017;32:176-88.
  74. Mascalchi M, Attina D, Bertelli E, et al. Lung cancer associated with cystic airspaces. *J Comput Assist Tomogr* 2015;39:102-8.
  75. Gurney JW, Lyddon DM, McKay JA. Determining the likelihood of malignancy in solitary pulmonary nodules with Bayesian analysis. Part II. Application. *Radiology*

- 1993;186:415-22.
76. Swensen SJ, Silverstein MD, Ilstrup DM, et al. The probability of malignancy in solitary pulmonary nodules. Application to small radiologically indeterminate nodules. *Arch Intern Med* 1997;157:849-55.
  77. Balekian AA, Silvestri GA, Simkovich SM, et al. Accuracy of clinicians and models for estimating the probability that a pulmonary nodule is malignant. *Ann Am Thorac Soc* 2013;10:629-35.
  78. Swensen SJ, Silverstein MD, Edell ES, et al. Solitary pulmonary nodules: clinical prediction model versus physicians. *Mayo Clin Proc* 1999;74:319-29.
  79. van Riel SJ, Ciompi F, Jacobs C, et al. Malignancy risk estimation of screen- detected nodules at baseline CT: comparison of the PanCan model, Lung-RADS and NCCN guidelines. *Eur Radiol* 2017;27:4019-29.
  80. Foley F, Rajagopalan S, Raghunath SM, et al. Computer-Aided Nodule Assessment and Risk Yield Risk Management of Adenocarcinoma: The Future of Imaging? *Semin Thorac Cardiovasc Surg* 2016;28:120-6.
  81. Yi CA, Lee KS, Kim EA, et al. Solitary pulmonary nodules: dynamic enhanced multi-detector row CT study and comparison with vascular endothelial growth factor and microvessel density. *Radiology* 2004;233:191-9.
  82. Swensen SJ, Viggiano RW, Midthun DE, et al. Lung nodule enhancement at CT: multicenter study. *Radiology* 2000;214:73-80.
  83. Chae EJ, Song JW, Seo JB, et al. Clinical utility of dual-energy CT in the evaluation of solitary pulmonary nodules: initial experience. *Radiology* 2008;249:671-81.
  84. Ohno Y, Nishio M, Koyama H, et al. Solitary pulmonary nodules: Comparison of dynamic first-pass contrast-enhanced perfusion area-detector CT, dynamic first-pass contrast-enhanced MR imaging, and FDG PET/CT. *Radiology* 2015;274:563-75.
  85. Gould MK, Maclean CC, Kuschner WG, et al. Accuracy of positron emission tomography for diagnosis of pulmonary nodules and mass lesions: a meta-analysis. *JAMA* 2001;285:914-24.
  86. Fletcher JW, Kymes SM, Gould M, et al. A comparison of the diagnostic accuracy of 18F-FDG PET and CT in the characterization of solitary pulmonary nodules. *J Nucl Med* 2008;49:179-85. Erratum in: *J Nucl Med* 2008;49:353.
  87. Veronesi G, Bellomi M, Veronesi U, et al. Role of positron emission tomography scanning in the management of lung nodules detected at baseline computed tomography screening. *Ann Thorac Surg* 2007;84:959-65; discussion 965-6.
  88. Marom EM, Sarvis S, Herndon JE 2nd, et al. T1 lung cancers: sensitivity of diagnosis with fluorodeoxyglucose PET. *Radiology* 2002;223:453-9.
  89. Erasmus JJ, McAdams HP, Patz EF Jr, et al. Evaluation of primary pulmonary carcinoid tumors using FDG PET. *AJR Am J Roentgenol* 1998;170:1369-73.
  90. Yap CS, Schiepers C, Fishbein MC, et al. FDG-PET imaging in lung cancer: how sensitive is it for bronchioloalveolar carcinoma? *Eur J Nucl Med Mol Imaging* 2002;29:1166-73.
  91. Demir Y, Polack BD, Karaman C, et al. The diagnostic role of dual-phase (18)F-FDG PET/CT in the characterization of solitary pulmonary nodules. *Nucl Med Commun* 2014;35:260-7.
  92. Kesner AL, Chung JH, Lind KE, et al. Validation of Software Gating: A Practical Technology for Respiratory Motion Correction in PET. *Radiology* 2016;281:239-48.

**Cite this article as:** Vlahos I, Stefanidis K, Sheard S, Nair A, Sayer C, Moser J. Lung cancer screening: nodule identification and characterization. *Transl Lung Cancer Res* 2018;7(3):288-303. doi: 10.21037/tlcr.2018.05.02